ORIGINAL ARTICLE: NEONATAL LUNG DISEASE

In silico numerical simulation of ventilator settings during high-frequency ventilation in preterm infants

Kai M. Förster MD[1,2] ⓘ | Christian J. Roth PhD[3] | Anne Hilgendorff MD[1,2,4] | Birgit Ertl-Wagner MD[5,6,7] | Andreas W. Flemmer MD[1] | Wolfgang A. Wall PhD[3]

[1]Division of Neonatology, Dr. von Hauner Children's Hospital, LMU University Hospital Munich, Munich, Germany

[2]Institute for Lung Biology and Disease and Comprehensive Pneumology Center with the CPC-M bioArchive, Helmholtz Zentrum München, Germany

[3]Institute for Computational Mechanics, Technical University of Munich, Garching, Germany

[4]Center for Comprehensive Developmental Care (CDeCLMU), LMU University Hospital Munich, Munich, 80337, Germany

[5]Department of Radiology, LMU University Hospital Munich, Munich, Germany

[6]Department of Diagnostic Imaging, The Hospital for Sick Children, Toronto, Canada

[7]Department of Medical Imaging, University of Toronto, Toronto, Canada

Correspondence
Andreas W. Flemmer, Division of Neonatology, Dr. von Hauner Children's Hospital, Perinatal Center, LMU Munich, Marchioninistrasse 15, 81337 Munich, Germany.
Email: Andreas.Flemmer@med.uni-muenchen.de

Abstract

Objective: Despite the routine use of antenatal steroids, exogenous surfactants, and different noninvasive ventilation methods, many extremely low gestational age neonates, preterm, and term infants eventually require invasive ventilation. In addition to prematurity, mechanical ventilation itself can induce ventilator-induced lung injury leading to lifelong pulmonary sequelae. Besides conventional mechanical ventilation, high-frequency oscillatory ventilation (HFOV) with tidal volumes below dead space and high ventilation frequencies is used either as a primary or rescue therapy in severe neonatal respiratory failure.

Methods and Results: Applying a high-resolution computational lung modeling technique in a preterm infant, we studied three different high-frequency ventilation settings as well as conventional ventilation (CV) settings. Evaluating the computed oxygen delivery (OD) and lung mechanics (LM) we outline for the first time how changing ventilator settings from CV to HFOV lead to significant improvements in OD and LM.

Conclusion: This personalized "digital twin" strategy advances our general knowledge of protective ventilation strategies in neonatal care and can support decisions on various modes of ventilatory therapy at high frequencies.

KEYWORDS
bronchopulmonary dysplasia, high-frequency oscillatory ventilation, mechanical ventilation, numeric simulation, preterm infant

Kai M. Förster and Christian J. Roth contributed equally as first authors.
Andreas W. Flemmer and Wolfgang A. Wall contributed equally as senior authors.

1 | INTRODUCTION

During conventional mechanical ventilation pulmonary gas exchange is maintained by direct alveolar aeration, applying tidal volume to the anatomical dead space, the large airways, and the alveolar compartment. Tidal volumes at or below the anatomical dead space during CV lead to deterioration of ventilation through CO_2-accumulation and may subsequently even impair oxygenation by atelectasis formation. In contrast, high-frequency oscillatory ventilation (HFOV) provides an effective approach for oxygenation by applying optimal mean airway pressures (MAPs) paired with low tidal volumes.

The underlying flow principle was observed in 1915 by Henderson and the method was initially described in detail by Lunkenheimer in the early 1970s.[1] Since then, HFOV has been continually developed[2,3] and is implemented in numerous ventilators, especially in those designed for mechanical ventilation of preterm infants. HFOV has been shown to result in better oxygenation[4] as well as long-term lung function[5,6] when compared to conventional ventilation (CV).

Potential mechanisms of gas exchange explaining oxygen delivery (OD) to the terminal lung regions in HFOV have been described previously, in particular, by Slutsky et al.,[7] Chang,[8] Venegas et al.,[3] and Pillow.[2] Computational methods have been used to simulate airflow and gas transport during HFOV and to elucidate its efficiency in oxygen and CO_2 transport. While providing important first insights, these computational methods have not been applicable to investigations on HFOV in the preterm infant: Herrmann et al.[9] investigated gas transport during HFOV in the canine lung. Further studies were limited to artificial or imaging-based adult airway tree geometries.[10,11] In our own recent work,[12] we have provided evidence for six out of eight mechanisms of gas exchange during HFOV in preterm infants as described by Slutsky et al.[7] The bronchial anatomy used in our model was derived from high-resolution magnetic resonance imaging (MRI) of a preterm infant and comprises the first seven generations of the bronchial tree as well as the used, nonblocked endotracheal tube. Infant lung function testing (ILFT) results are included to respect the lung mechanics (LM) of the patient.

With the described, high-resolution computational model derived from in vivo measurements of one patient in hands, we are now capable of modifying ventilator settings for a specific clinical situation in in silico (by computational modeling) in a defined environment and under controlled conditions. These prerequisites are usually not feasible in a clinical setting and result from experimental data are not easily translated to preterm infants.

We aimed to compare the effect of different ventilator settings during HFOV and CV on OD and LM, that is, compliance in neonatal airways of a preterm infant. Therefore, we investigated the impact of frequency and MAP, which are the main parameters for controlling oxygenation and providing an optimal ventilation–perfusion ratio.

2 | MATERIALS AND METHODS

2.1 | Patient characteristics

A preterm infant from the AIRR study cohort (Attention to Infants @ Respiratory Risk) with later development of bronchopulmonary dysplasia (BPD) born at 27 3/7 weeks of gestation at the Perinatal Center of the University Hospital, LMU Munich, was chosen for all investigations in this study. While performing pulmonary MRI and lung function tests, the infant was breathing spontaneously in room air (FiO_2 0.21). Further patient characteristics are given in Table 1. Approval by the local Ethics Committee and written informed parental consent for the study infant was obtained (Munich cohort #195-07; German Registry for Clinical Studies DRKS00004600). All methods were performed in accordance with the relevant guidelines and regulations of the local Ethics Committee and the declaration of Helsinki.

2.2 | ILFT at 36 weeks GA

ILFT was performed at 36 weeks GA under light sedation with chloral hydrate (30 mg/kg) in the supine position. The Jaeger MasterScreen BabyBody device (v4.6; CareFusion) was used for the pulmonary function measurement, with Rendell-Baker Soucek face masks (size: 0 or 1; Rüsch UK Ltd.).

An air-tight seal was achieved using a rim of therapeutic putty (cosiMed). Heart rate and SpO_2 were monitored continuously throughout testing and emergency equipment was kept at hand. Measurements were standardized according to the recommendations of the American Thoracic Society and European Respiratory Society.[14,15] Measurements of tidal breathing, passive respiratory mechanics, and functional residual capacity (FRC_p) were performed. Total respiratory compliance (C_{rs}) was assessed in the single-occlusion technique under a stable end-expiratory level before activating the balloon shutter. FRC_p was measured in the body plethysmograph as described previously with the infant making respiratory efforts against a closed shutter.[16,17] For our patient, a C_{rs} of 20.93 ml/kPa

TABLE 1 Patient characteristics of the preterm infant investigated in this study

BPD grade	3
Gestational age (weeks PMA)	27.3
Birth weight (g)	760
Days of mechanical ventilation	78
Endotracheal mechanical ventilation (n/days)	32
Pharyngeal ventilation/CPAP (n/days)	46
ICU stay (days)	103

Abbreviations: BPD, bronchopulmonary dysplasia, according to Jobe and Bancalari[13]; CPAP, continuous positive airway pressure; ICU, intensive care unit; PMA, postmenstrual age.

was determined and used in lung model simulation. All references to body weight refer to a weight of 3.3 kg at the time of the examination.

2.3 | Pulmonary MRI at 36 weeks GA

Pulmonary noncontrast-enhanced MRI was performed in nonsedated, spontaneous sleep in the supine position in a 3-Tesla whole-body MRI scanner (Magnetom Skyra, Siemens Healthineers). MRI was performed with a size-adapted number of coil elements from the 32-channel spine array coil, an 18-channel flexible body array coil, and the 20-channel head-and-neck array coil. The protocol included pulse sequences for the qualitative and quantitative assessment of morphology, volume, and structural changes of the lung. For lung geometry extraction in this study, a T1-weighted magnetization-prepared rapid gradient-echo sequence with an image size of $256 \times 256 \times 144 px^3$ was chosen.

2.4 | Computed ventilator settings

A three-dimensional computational model of the infant's lung was built based upon the 3 Tesla infant lung MRI mimicking the regional LM acquired from ILFT. Using this model, airflow and gas transport to the distal lung regions can be simulated.

Within our lung model,[12] an unblocked endotracheal tube with an inner diameter of 3.0 mm was simulated in the trachea according to clinical guidelines. An observed tube leakage of approximately 15% of the supplied tidal volume is in line with clinical findings.[18] Further details of the in silico lung model are described in the paper by Roth et al.[12] Three different ventilator settings during HFOV (in silico high-frequency [HF] ventilation setting-1, HF-2, and HF-3) were compared with each other as well as to a standard CV setting and computed in the digital twin model to study their effects on oxygenation and LM.

Ventilator settings were chosen to explore the spectrum of the model and to cover possible clinical respirator settings (Table 2):

2.4.1 | In silico HF-1

A MAP of 8 cmH$_2$O was constantly applied to the airway opening. Furthermore, a combination of two sinusoidal flow rate curves was simulated to be superimposed during the inflation phase with a frequency of $f = 10$ Hz, a tidal volume of $V_T = 2.0$ ml/kg body weight, and an inspiratory/expiratory ratio of I:E = 1:2. The expiratory flow was allowed to freely develop depending on the regional LM calculated from ILFT, that is, R_{eq}^i and C_{eq}^i, and the applied MAP.

2.4.2 | In silico HF-2

Equal settings and minute volume as HF-1 with a frequency decreased to 7 Hz. A tidal volume of $V_T = 2.86$ ml/kg body weight was applied.

TABLE 2 Simulated ventilator settings for three modes of high-frequency (HF) ventilation and a mode of conventional ventilation (CV)

	HF-1	HF-2	HF-3	CV
Frequency (Hz)	10	7	10	~60 (1/min)
Tidal volume (ml/kg)	2	2.86	2	5
MAP (cmH$_2$O)	8	8	12	6
Minute volume (TV × f, ml/s)	66	66	66	18
I:E	1:2	1:2	1:2	1:2
Tube leakage	15%	15%	15%	15%
FiO$_2$	0.35	0.35	0.35	0.35
Simulated cycles	8	8	8	2

Abbreviations: E, expiration; FiO$_2$, volume fraction of inspired oxygen; I, inspiration; MAP, mean airway pressure.

2.4.3 | In silico HF-3

Equal settings as HF-1 with an increased MAP of 12 cmH$_2$O. A tidal volume of $V_T = 2.0$ ml/kg body weight was applied.

2.4.4 | In silico CV

Ventilator rate of 60/min, a tidal volume of 5.0 ml/kg body weight, a positive end-expiratory pressure (PEEP) of 6 cmH$_2$O, and an inspiratory/expiratory ratio of I:E = 1:2 were applied.

3 | RESULTS

The computed amount of oxygen leaving the respiratory tree at the peripheral lung tissue site (O$_2$, out) is assumed to be available for gas exchange in the lung tissue in all tested ventilator settings. To be able to compare different HF settings of the ventilator, the amount of oxygen (O$_2$, out) provided to the lung tissue for gas exchange was normalized to a duration of 1 min, based on the respiratory cycles that have been computed. Minute ventilation was equal for all HF settings (Table 2).

3.1 | OD to lung tissue in HFOV and conventional mechanical ventilation

3.1.1 | HF-1

Applying a MAP of 8 cmH$_2$O in HF-1, the amount of oxygen (O$_2$, out) leaving the respiratory tree is 1.14 ml O$_2$ following one oscillation (Figure 1). Again, referencing the oxygen supply to 1 min, the amount of oxygen (O$_2$, out) leaving the respiratory tree at the peripheral lung tissue site is 684 ml O$_2$/min. This amount
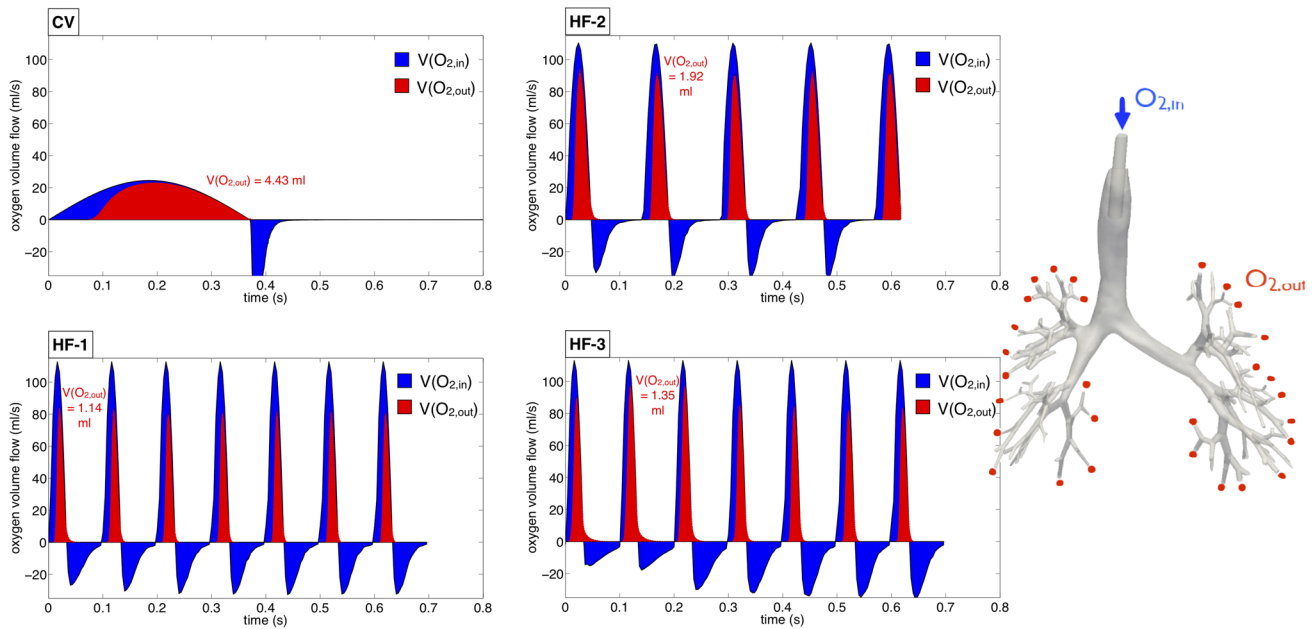
FIGURE 1 Summary of oxygen provided at the inlet (O2, in; blue) and the oxygen arriving at the lung tissue (O2, out; red). The curves indicate the flow and the area under the curve the volume of oxygen. The graphs are shown for the conventional ventilation (CV) and the HF-1, HF-2, and HF-3 settings. The computed amount of oxygen leaving the respiratory tree at the peripheral lung tissue site (O2, out) is assumed to be available for gas exchange in the lung tissue in all tested ventilator settings. To be able to compare different high-frequency (HF) settings of the ventilator, the amount of oxygen (O2, out) provided to the lung tissue for gas exchange was normalized to a duration of 1 min, based on the respiratory cycles that have been computed. Minute ventilation was equal for all HF settings (Table 2) [Color figure can be viewed at wileyonlinelibrary.com]

represents 49% of the 1386 ml O_2/min provided at the airway opening at a FiO_2 of 0.35 (O_2, in).

3.1.2 | HF-2

Applying a frequency of 7 Hz in HF-2, the amount of oxygen (O_2, out) leaving the respiratory tree is 1.92 ml O_2 following one oscillation (Figure 1). Referencing the oxygen supply to 1 min, the amount of oxygen (O_2, out) leaving the respiratory tree at the peripheral lung tissue site is 807 ml O_2/min. This corresponds to 58% of the provided oxygen at the airway opening at a FiO_2 of 0.35.

3.1.3 | HF-3

Applying a MAP of 12 cmH$_2$O in HF-3, the amount of oxygen (O_2, out) leaving the respiratory tree is 1.35 ml O_2 following one oscillation (Figure 1). Referencing the oxygen supply to 1 min, the amount of oxygen (O_2, out) leaving the respiratory tree at the peripheral lung tissue site is 810 ml O_2/min corresponding to 58% of the provided oxygen at the opening at a FiO_2 of 0.35.

During CV with a set tidal volume of 5 ml/kg body weight the amount of oxygen (O_2, out) leaving the respiratory tree after one ventilation cycle was 4.43 ml O_2 (Figure 1). As a result, 265 ml O_2/min is delivered to the tissue. This amount represents 76% of the 346 ml O_2/min provided at the airway opening at a FiO_2 of 0.35.

Comparing the three HF settings, there is a 9% increased uptake of oxygen offered to lung tissue (O_2, out) by a reduction of the frequency of 30% in HF-2 as well as a 9% improvement in OD to the lung tissue (O_2, out) by increasing the MAP for 50% in HF-3.

3.2 | HFOV requires low peak airway pressure to drive ventilation

Additional ventilation parameters extracted from the simulated scenarios are (i) peak airway pressure and (ii) pressure difference between maximum inspiration and expiration.

3.2.1 | HF-1

In the HF-1 setting, a MAP of 8 cmH$_2$O is applied, that is, 2 cmH$_2$O more than PEEP in the CV setting. The pressure difference required to achieve the targeted tidal volume is 1.6 cmH$_2$O, resulting in a maximum airway pressure of 9.6 cmH$_2$O, similar to the CV setting.

3.2.2 | HF-2

In the HF-2 setting, a MAP of 8 cmH$_2$O is applied. To achieve an equal minute volume as in HF-1, yet with a lower frequency, a
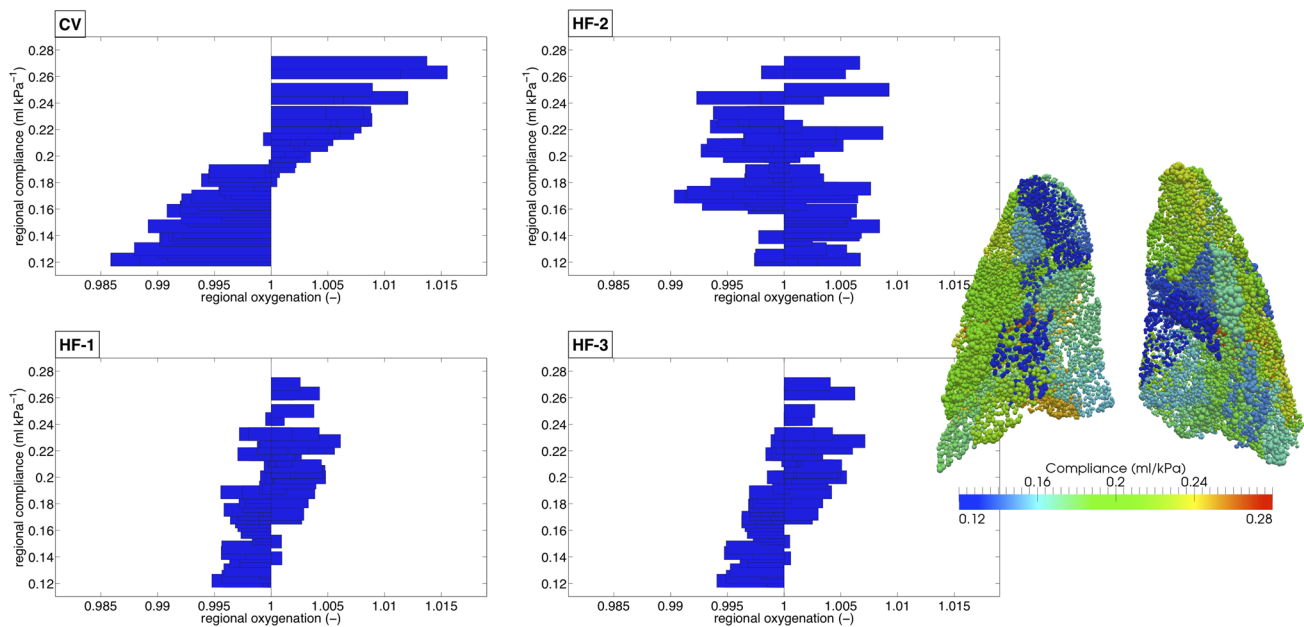
FIGURE 2 Regional distribution of oxygen in comparison with the regional lung compliance. The compliance is deduced from the magnetic resonance imaging scan by the method outlined by Roth et al.[12] The regional oxygenation is referenced to the mean oxygenation and multiplied by 1/128 (number of outlets) of the entire oxygen delivery in the current setting. The conventional ventilation (CV) setting shows that regional compliance and regional oxygenation are directly linked and that higher compliance automatically leads to higher oxygenation in that area. In the case of the high-frequency (HF) settings, regional oxygenation and compliance become partially decoupled and high compliance does not automatically lead to high inflation in that area [Color figure can be viewed at wileyonlinelibrary.com]

pressure difference of 3.3 cmH$_2$O between maximum inspiration and expiration is required. The resulting maximum airway pressure is 11.3 cmH$_2$O.

3.2.3 | HF-3

The HF-3 setting is similar to the HF-1 setting, but with an increased MAP of 12 cmH$_2$O. The pressure difference to drive ventilation is 1.8 cmH$_2$O, resulting in a maximum airway pressure of 13.8 cmH$_2$O at end inspiration.

The highest maximum airway pressure results in the HF-3 setting with 13.8 cmH$_2$O, while a pressure difference of 3.3 cmH$_2$O between maximum inspiration and expiration represents the highest pressure difference in all in silico HF settings.

3.3 | CV requires high peak airway pressure to drive ventilation

During CV modeling, a PEEP of 6 cmH$_2$O was used and a pressure difference of 3.5 cmH$_2$O was required to drive the airflow within the given inspiratory time until the 5 ml/kg of tidal volume was achieved. This leads to a maximum airway pressure of 9.5 cmH$_2$O at the time of end inspiration.

The CV setting requires a high-pressure difference between inhalation and exhalation referenced to the amount of provided oxygen.

3.4 | HFOV shows a more homogeneous distribution of oxygen in comparison to conventional frequency

The illustration of the volume fraction of oxygen in the individual pulmonary segments is visualized in Figures 2 and 3. In Figure 2 the regional oxygenation is shown relative to the compliance of the respective lung region. The parameter "regional oxygenation" is referenced to the mean oxygenation and multiplied by 1/128 (number of outlets) of the entire OD in the current setting.

The CV scenario shows that regional compliance and regional oxygenation are directly linked. Pulmonary segments with higher compliance than the average compliance of 0.19 ml/kPa exhibit higher regional oxygenation. In the case of the HF settings, regional oxygenation becomes more homogeneous and high compliance in one single region does not automatically lead to high inflation in that area.

In Figure 3, the computed oxygenation is superimposed on the infant's MRI. For CV oxygenation, CV shows areal hotspots indicated by dark red color whereas oxygenation in all HF settings is more homogeneously distributed at a medium level throughout the lung (pale red color).

4 | DISCUSSION

Using cutting edge in silico modeling, we simulated for the first time the effects of different ventilator settings during HFOV and CV for a preterm infant by generating a model based on a patient's individual
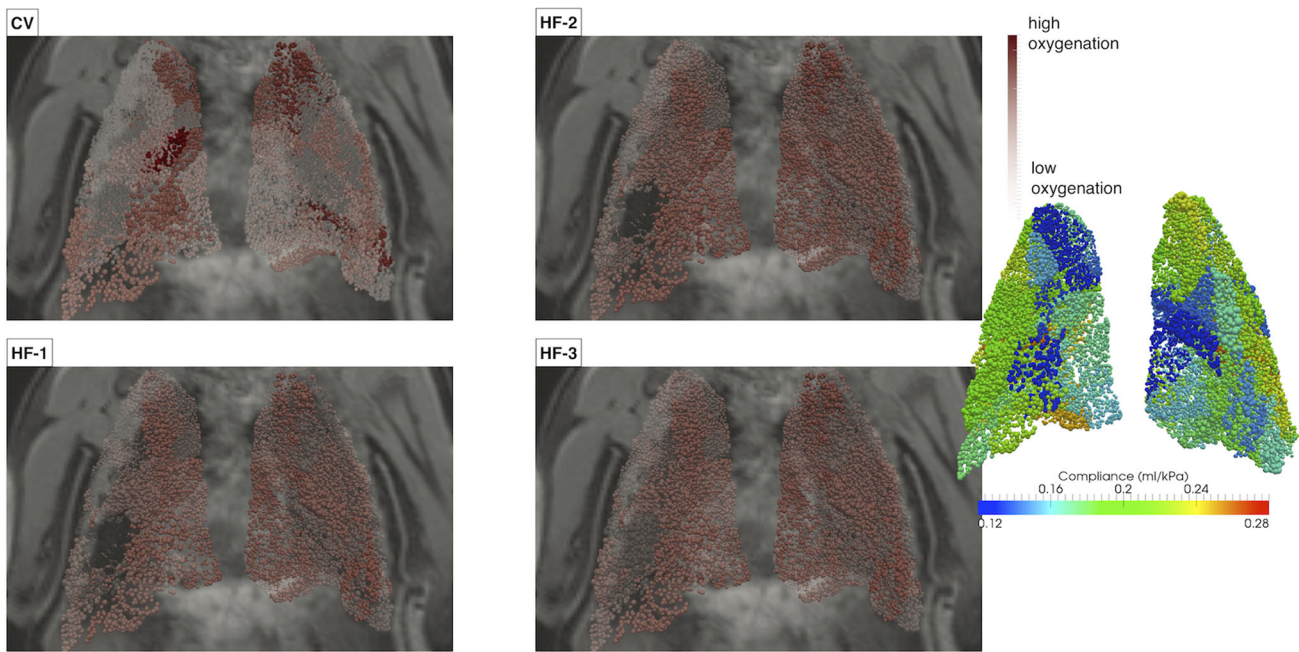
FIGURE 3 Regional oxygenation is visualized as an oxygenation "heat map." Areas with high oxygenation are visualized in red and those with low oxygenation are shown as transparent. In the conventional ventilation (CV) scenario there are "hotspots" with high oxygenation corresponding to the regions with high compliance. In the high-frequency (HF) scenarios, the "hotspots" disappear, resulting in a more homogeneous oxygenation [Color figure can be viewed at wileyonlinelibrary.com]

airway morphology and LM and thus creating a virtual "digital twin." Slutsky et al.[7] proposed alternative mechanisms of gas exchange such as molecular diffusion, Taylor dispersion, turbulence, asymmetric velocity profiles, Pendelluft, cardiogenic mixing, and collateral ventilation in HFOV. Previously, our computational approach[12] has provided evidence for six of these gas exchange mechanisms, explaining OD to the terminal lung regions for tidal volumes much smaller than respiratory dead space.

The first clinical trials comparing invasive ventilation strategies that used conventional respiration rates and HFOV yielded no difference in outcome.[19,20] Nonetheless, higher rates of intraventricular hemorrhage (IVH) were suspected in the HFOV-treated infants,[19] contradicted by studies such as the UKOS trial, which demonstrated no difference in survival or complications (chronic lung disease and death) but a reduction in IVH severity under HFOV treatment.[21] Underscoring potential benefits, the Neonatal Ventilation Study Group demonstrated earlier weaning from respiratory support and less oxygen supplementation at discharge in infants ventilated with HFOV.[22] In line with this, the follow-up of the UKOS trial showed superior lung function at 11–14 years, with no evidence of poorer functional outcomes in those infants who had undergone HFOV, as compared to those who had received CV.[6] Primarily based on these data, HFOV is currently suggested as rescue therapy for respiratory distress syndrome and acute respiratory distress syndrome as it could reduce ventilator-induced lung injury (VILI)[7,23] without serious side effects if overinflation is avoided. As results from clinical studies are not conclusive, the latest Cochrane review from 2015 gave no recommendation for the routine use of HFOV in premature infants with respiratory distress[5] so that its rescue character remains.

In our current study, four different ventilation profiles—one CV and three HF settings—were tested in our in silico patient lung model[12]: as early as 1 min after initiation of ventilation, the oxygen volume provided to the lung tissue is the highest for HF-3 (810 ml/min) while the degree of efficiency is higher within the CV setting (76% of the oxygen provided at the airway opening is available to the lung tissue vs. 58% in HF-2 + 3 vs. 49% in HF-1). These results have to be taken into account when reflecting on current treatment practices that aim to achieve a shorter duration of invasive ventilation strategies[24,25] at the cost of prolonged exposure to supplemental oxygen.[26,27]

Increasing the absolute amount of oxygen provided to lung tissue is almost not possible in a CV setting due to the risk of VILI.[28–30] Currently, the pressure levels in HF-3 are 13.8 cmH$_2$O and in CV at a maximum of 9.5 cmH$_2$O. To increase the effectiveness of OD to 810 ml/min (HF-3) in distal lung regions—on the basis of a different provided minute ventilation—the maximum pressure would need to be increased to 16.7–3 cmH$_2$O higher than in the HF-3. HFOV, therefore, delivers a significantly increased amount of oxygen to the alveolar region at a lower pressure difference compared to CV. These considerations could be of importance when discussing the effects of VILI[28–30] in the induction of chronic complications, such as BPD.[31]

The most significant insight into LM here is that OD during HFOV occurs more homogenously than during CV. In CV, regional tissue aeration/inflation is mainly governed by regional tissue compliance (see Figure 2). This means regions with high compliance show a tendency toward inflation/overinflation while regions with low compliance exhibit almost no inflation at all. This pattern is visualized by the linear increase in the compliance/oxygenation diagram in

Figure 2 (CV). In contrast, the HFOV settings show a strong tendency toward a "rectangular block" picture, indicating that all regions, independent of the compliance, are ventilated uniformly. This would indicate an outcome in ventilator therapy that could be very beneficial in the management of neonates with ventilation–perfusion mismatch.[32]

Overinflation, however, also occurs in this setting especially in regions showing extremely high compliance. Figure 3 visualizes the regions at specific risk for overinflation and again outlines the homogenized regional oxygenation during HFOV.

There are limitations to our study that need to be considered when interpreting the data. First, the medical imaging data used in this study were obtained from a preterm infant at the age of 3 months. This might underestimate the flow situation in an extremely preterm (and even smaller) neonate subjected to HFOV early during the clinical course. Furthermore, even though the focus of the present work lies in the evaluation of OD, our future goal is to investigate the entire gas exchange, including CO_2 elimination. This is dependent on several parameters, most notably the perfusion. We plan to address this topic by modeling echocardiography data in the next step. The clinical applicability of our model is currently curtailed as we are dealing with a heterogeneous patient population with respect to the disease process[33,34] and the range of ventilators capable of performing HFOV, not to mention the expertise of the users who operate them, is limited.[23] Investigating the above-mentioned effects, along with a larger number of breathing cycles is technically possible but currently limited by the computational cost is required to investigate HFOV phenomena at such a level of detail.

Even though we currently examine selected ventilator settings ($n = 4$), a significant advantage of our work lies in our maintaining the same basic conditions within the framework of numerical simulation and our ability to isolate interference effects. In addition, we have adequate plausibility checks in our modeling process.[12]

Beyond that, the difficulties of invasive measurements and sequential medical imaging, especially in the preterm infant, are overcome by means of our numerical approach using an advanced computational lung model based on the real anatomy and physiology of the infant's lung. This detailed insight into HFOV in terms of supplied oxygen, pressure, and homogeneity (higher homogeneity in HF settings compared to CV) provides a better understanding of this ventilation technique.

In conclusion, we are now capable of modifying ventilator settings for a specific clinical situation in in silico and may even predict the effect of these setting changes on oxygenation, supporting relevant clinical studies such as those from Hofemeier et al.[35] as well as Miedema et al.[36] The computational model allows the targeting of single parameter changes, and we demonstrated the effect of variation in tidal volume, frequency, and MAP. These insights pave the way for developing optimal ventilatory assistance strategies for the immature lung, may thus facilitate more robust recommendations regarding the application of HFOV, and, finally, can serve as a hypothesis generator for clinical trials.

CONFLICT OF INTERESTS

The authors declare that there are no conflict of interests.

AUTHOR CONTRIBUTIONS

Christian J. Roth and Kai M. Förster performed the analysis. Kai M. Förster, Christian J. Roth, Wolfgang A. Wall, and Andreas W. Flemmer designed the study. Kai M. Förster, Anne Hilgendorff, and Birgit Ertl-Wagner were responsible for patient recruitment and medical imaging. Christian J. Roth and Kai M. Förster prepared figures and tables. Kai M. Förster, Christian J. Roth, Wolfgang A. Wall, and Andreas W. Flemmer wrote the manuscript.

DATA AVAILABILITY STATEMENT

Data are available on request from the authors.

ORCID

Kai M. Förster https://orcid.org/0000-0002-4127-1400

REFERENCES

1. Lunkenheimer PP, Rafflenbeul W, Keller H, Frank I, Dickhut HH, Fuhrmann C. Application of transtracheal pressure oscillations as a modification of "diffusing respiration". *Br J Anaesth.* 1972;44(6):627.
2. Pillow JJ. High-frequency oscillatory ventilation: mechanisms of gas exchange and lung mechanics. *Crit Care Med.* 2005;33(3 suppl): S135-S141.
3. Venegas JG, Fredberg JJ. Understanding the pressure cost of ventilation: why does high-frequency ventilation work? *Crit Care Med.* 1994;22(9 suppl):S49-S57.
4. Imai Y, Slutsky AS. High-frequency oscillatory ventilation and ventilator-induced lung injury. *Crit Care Med.* 2005;33(3 suppl):S129-S134.
5. Cools F, Offringa M, Askie LM. Elective high frequency oscillatory ventilation versus conventional ventilation for acute pulmonary dysfunction in preterm infants. *Cochrane Database Syst Rev.* 2015;(3):CD000104. https://doi.org/10.1002/14651858.CD000104.pub4
6. Zivanovic S, Peacock J, Alcazar-Paris M, et al. Late outcomes of a randomized trial of high-frequency oscillation in neonates. *N Engl J Med.* 2014;370(12):1121-1130.
7. Slutsky AS, Drazen JM. Ventilation with small tidal volumes. *N Engl J Med.* 2002;347(9):630-631.
8. Chang HK. Mechanisms of gas transport during ventilation by high-frequency oscillation. *J Appl Physiol Respir Environ Exerc Physiol.* 1984;56(3):553-563.
9. Herrmann J, Tawhai MH, Kaczka DW. Regional gas transport in the heterogeneous lung during oscillatory ventilation. *J Appl Physiol.* 2016;121(6):1306-1318.
10. Bauer K, Rudert A, Brucker C. Three-dimensional flow patterns in the upper human airways. *J Biomech Eng.* 2012;134(7):071006.
11. Choi J, Xia G, Tawhai MH, Hoffman EA, Lin CL. Numerical study of high-frequency oscillatory air flow and convective mixing in a CT-based human airway model. *Ann Biomed Eng.* 2010;38(12):3550-3571.
12. Roth CJ, Forster KM, Hilgendorff A, Ertl-Wagner B, Wall WA, Flemmer AW. Gas exchange mechanisms in preterm infants on HFOV—a computational approach. *Sci Rep.* 2018;8(1):13008.

13. Jobe AH, Bancalari E. Bronchopulmonary dysplasia. *Am J Respir Crit Care Med*. 2001;163(7):1723-1729.

14. Hulskamp G, Pillow JJ, Dinger J, Stocks J. Lung function tests in neonates and infants with chronic lung disease of infancy: functional residual capacity. *Pediatr Pulmonol*. 2006;41(1):1-22.

15. Stocks J, Godfrey S, Beardsmore C, Bar-Yishay E, Castile R. Plethysmographic measurements of lung volume and airway resistance. ERS/ATS Task Force on Standards for Infant Respiratory Function Testing. European Respiratory Society/American Thoracic Society. *Eur Respir J*. 2001;17(2):302-312.

16. Menache MG, Hofmann W, Ashgarian B, Miller FJ. Airway geometry models of children's lungs for use in dosimetry modeling. *Inhal Toxicol*. 2008;20(2):101-126.

17. Nguyen TT, Hoo AF, Lum S, Wade A, Thia LP, Stocks J. New reference equations to improve interpretation of infant lung function. *Pediatr Pulmonol*. 2013;48(4):370-380.

18. Mahmoud RA, Proquitte H, Hadhood SE, Schmalisch G. Effect of endotracheal tube leakage on respiratory function monitoring: comparison of three neonatal ventilators. *J Pediatr Intensive Care*. 2012;1(2):61-69.

19. The HIFI Study Group. High-frequency oscillatory ventilation compared with conventional mechanical ventilation in the treatment of respiratory failure in preterm infants. *N Engl J Med*. 1989;320(2):88-93.

20. Thome U, Kössel H, Lipowsky G, et al. Randomized comparison of high-frequency ventilation with high-rate intermittent positive pressure ventilation in preterm infants with respiratory failure. *J Pediatr*. 1999;135(1):39-46.

21. Johnson AH, Peacock JL, Greenough A, et al. High-frequency oscillatory ventilation for the prevention of chronic lung disease of prematurity. *N Engl J Med*. 2002;347(9):633-642.

22. Courtney SE, Durand DJ, Asselin JM, et al. High-frequency oscillatory ventilation versus conventional mechanical ventilation for very-low-birth-weight infants. *N Engl J Med*. 2002;347(9):643-652.

23. Meyers M, Rodrigues N, Ari A. High-frequency oscillatory ventilation: a narrative review. *Can J Respir Ther*. 2019;55:40-46.

24. Fischer HS, Buhrer C. Avoiding endotracheal ventilation to prevent bronchopulmonary dysplasia: a meta-analysis. *Pediatrics*. 2013;132(5):e1351-e1360.

25. Subramaniam P, Ho JJ, Davis PG. Prophylactic nasal continuous positive airway pressure for preventing morbidity and mortality in very preterm infants. *Cochrane Database Syst Rev*. 2016;(6):CD001243. https://doi.org/10.1002/14651858.CD001243.pub3

26. Davidson LM, Berkelhamer SK. Bronchopulmonary dysplasia: chronic lung disease of infancy and long-term pulmonary outcomes. *J Clin Med*. 2017;6(1):4.

27. Manja V, Lakshminrusimha S, Cook DJ. Oxygen saturation target range for extremely preterm infants: a systematic review and meta-analysis. *JAMA Pediatr*. 2015;169(4):332-340.

28. Beitler JR, Malhotra A, Thompson BT. Ventilator-induced lung injury. *Clin Chest Med*. 2016;37(4):633-646.

29. Jobe AH. The new bronchopulmonary dysplasia. *Curr Opin Pediatr*. 2011;23:167-172.

30. van Kaam AH, De Luca D, Hentschel R, et al. Modes and strategies for providing conventional mechanical ventilation in neonates [published online ahead of print November 30, 2019]. *Pediatr Res*. https://doi.org/10.1038/s41390-019-0704-1

31. Ambalavanan N, Carlo WA. Ventilatory strategies in the prevention and management of bronchopulmonary dysplasia. *Semin Perinatol*. 2006;30(4):192-199.

32. Lakshminrusimha S. The pulmonary circulation in neonatal respiratory failure. *Clin Perinatol*. 2012;39(3):655-683.

33. Siffel C, Kistler KD, Lewis JFM, Sarda SP. Global incidence of bronchopulmonary dysplasia among extremely preterm infants: a systematic literature review. *J Matern Fetal Neonatal Med*. 2019;34:1721-1731.

34. Thébaud B, Goss KN, Laughon M, et al. Bronchopulmonary dysplasia. *Nat Rev Dis Primers*. 2019;5(1):78.

35. Hofemeier P, Shachar-Berman L, Tenenbaum-Katan J, Filoche M, Sznitman J. Unsteady diffusional screening in 3D pulmonary acinar structures: from infancy to adulthood. *J Biomech*. 2016;49(11):2193-2200.

36. Miedema M, de Jongh FH, Frerichs I, van Veenendaal MB, van Kaam AH. The effect of airway pressure and oscillation amplitude on ventilation in pre-term infants. *Eur Respir J*. 2012;40(2):479-484.